Food and Chemical Toxicology 178 (2023) 113925

Contents lists available at ScienceDirect

Food and Chemical Toxicology

journal homepage: www.elsevier.com/locate/foodchemtox

Butyric acid inhibits oxidative stress and inflammation injury in calcium oxalate nephrolithiasis by targeting CYP2C9

Zijian Zhou [a,b,1], Xuan Zhou [c,1], Yu Zhang [d,1], Yuanyuan Yang [a,b], Lujia Wang [a,b,*], Zhong Wu [a,b,**]

[a] Department of Urology, Huashan Hospital, Fudan University, Shanghai, 200040, PR China
[b] Clinical Research Center of Urolithiasis, Shanghai Medical College, Fudan University, Shanghai, 200040, PR China
[c] Department of Urology, The First Affiliated Hospital of Nanjing Medical University, Nanjing, 210029, PR China
[d] Department of Pharmacy, Huashan Hospital, Fudan University, Shanghai, 200040, PR China

ARTICLE INFO

Handling Editor: Dr. Bryan Delaney

Keywords:
Butyric acid
Calcium oxalate nephrolithiasis
Oxidative stress
Network pharmacology
CYP2C9

ABSTRACT

This study investigates the mechanism by which butyric acid can protect against calcium oxalate (CaOx) nephrolithiasis. To do so, a rat model was used with 0.75% ethylene glycol administration to induce CaOx crystal formation. Histological and von Kossa staining revealed calcium deposits and renal injury, while dihydroethidium fluorescence staining was used to detect reactive oxygen species (ROS) levels. Flow cytometry and TUNEL assays were used to assess apoptosis, respectively. Treatment with sodium butyrate (NaB) was found to partially reverse the oxidative stress, inflammation, and apoptosis associated with CaOx crystallization in the kidney. In addition, in HK-2 cells, NaB reversed the decreased cell viability, increased ROS levels and apoptosis damage caused by oxalate exposure. Network pharmacology was employed to predict the target genes of butyric acid, CYP2C9. Subsequently, NaB was found to significantly reduce CYP2C9 levels *in vivo* and *in vitro*, and inhibition of CYP2C9 by Sulfaphenazole (a specific CYP2C9 inhibitor), was able to reduce ROS levels, inflammation injury, and apoptosis in oxalate-induced HK-2 cells. Collectively, these findings suggest that butyric acid may inhibit oxidative stress and reduce inflammation injury in CaOx nephrolithiasis by suppressing CYP2C9.

1. Introduction

Nephrolithiasis is one of the most frequent pathologies of the urinary system which has imposed a significant economic burden and reduces the quality of life (Crivelli et al., 2021). Physicochemical studies have verified that most kidney stones are calcium oxalate (CaOx) stones (Knoll et al., 2011). CaOx nephrolithiasis is a prevalent and recurrent problem, thought to be the consequence of genetic, metabolic, environmental, and lifestyle elements (Fakhoury et al., 2019; Zisman et al., 2020). Current hypotheses propose that supersaturation and deposition of CaOx crystal in renal tissues contribute to kidney tubular cell apoptosis and injury, thus facilitating ongoing kidney stone formation (Witting et al., 2021). Other than specific pharmacological and surgery interventions, recommendations for lifestyle and nutritional changes can be pursued for preventive or therapeutic measures for CaOx stones (Rysz et al., 2021; Türk et al., 2016).

Short-chain fatty acids (SCFAs) were produced by anaerobic bacteria ferment dietary fiber in the intestinal tract, playing key roles not only in the local intestinal barrier but also at the systemic level (Schulthess et al., 2019). Recent research has revealed that the gut microbiota of renal stone patients contains a lower abundance of SCFA-producing bacteria (Liu et al., 2020). Butyric acid is one of the most abundant SCFAs and executes anti-inflammatory or immune-suppressive operations (Stoeva et al., 2021). Studies have revealed dysbiosis of butyric acid metabolism has been linked to several medical conditions like diabetes, cancer and kidney disease (Bayazid et al., 2022; Luzardo-Ocampo et al., 2020). However, few studies have explored the effect and the underlying target of butyric acid on CaOx nephrolithiasis to date.

Reactive oxygen species (ROS) are the primary agents responsible for oxidative damage, damaging the tubular cells and providing adhesive sites for CaOx crystals, thus promoting nephrolithiasis formation (Awuah Boadi et al., 2021; Khan, 2013; Shin et al., 2022). Cytochrome

* Corresponding author. Department of Urology, Huashan Hospital & Institute of Urology, Fudan University, Shanghai, 200040, PR China.
** Corresponding author. Department of Urology, Huashan Hospital & Institute of Urology, Fudan University, Shanghai, 200040, PR China.
E-mail addresses: lukewang2006@126.com (L. Wang), drzhongwu2020@163.com (Z. Wu).
[1] These authors have contributed equally to this work.

https://doi.org/10.1016/j.fct.2023.113925
Received 29 January 2023; Received in revised form 20 June 2023; Accepted 29 June 2023
Available online 4 July 2023
0278-6915/

P450s (CYPs), as monooxygenases, are essential for body metabolism and are capable of catalyzing the oxidation of a wide range of substrates (Zanger and Schwab, 2013). CYPs are primarily responsible for drug metabolism (Fukami et al., 2022). To date, no studies reported that CYPs are involved in calcium oxalate metabolism. Calcium oxalate metabolism primarily occurs through endogenous enzymes like alanine-glyoxylate aminotransferase (AGT), rather than CYPs directly (Danpure and Rumsby, 2004). However, it has been observed that CYPs can lead to the overproduction of ROS, thus initiating oxidative stress damage, which could be a trigger of CaOx crystals (Zhang et al., 2021). Inhibiting CYPs activation can offer protection to cells from ROS induced-damage (Zheng et al., 2019).

Our research aims to investigate the influence of butyric acid on the development of CaOx crystals, and to gain a basic understanding of the mechanism behind it. We found that butyric acid could inhibit oxidative stress and inflammation injury in the CaOx nephrolithiasis model both *in vitro* and *in vivo*. Then, we used network pharmacology for predictive work and selected CYP2C9 as the target gene of butyric acid impacting on CaOx nephrolithiasis. Finally, cell experiments were carried out to confirm the role of CYP2C9 in the oxalate-induced HK-2 cell injury model.

2. Materials and methods

2.1. CaOx stone model and treatment

Sprague-Dawley rats (5–6 weeks old, male) were acclimatized for 5 days prior to experiments. Fudan Laboratory Animal Ethics Board approved this study. Firstly, 18 rats were divided into 3 equal groups: the control group, the model group and the NaB group. Rats in the control group were allowed to drink sterile tap water freely while rats in the model group were administered 0.75% ethylene glycol (EG) in drinking water for 4 weeks. The NaB group received drinking water with 0.75% EG and 150 mM sodium butyrate (Liu et al., 2021). After 4 weeks, we collected blood plasma and renal tissues. Serum biomarkers of renal function were analyzed with an automatic biochemical analyzer (Servicebio, Wuhan, China) for the test.

2.2. Histologic analysis

Renal tissues were preserved in 10% formaldehyde, embedded in paraffin and cut into 5-μm slices for hematoxylin & eosin (HE), Von Kossa (VK), Alizarin Red (AR), and Masson staining. AR staining pH 6.8 can stain CaOx crystal and AR pH 4.3 stains CaP crystals (Proia and Brinn, 1985). Immunohistochemistry (IHC) was conducted to detect renal protein expression. Terminal deoxynucleotidyl transferase-mediated uridine triphosphate nick end-labeling (TUNEL) staining was performed to label the 3′-end of fragmented DNA in the apoptotic renal tissues, following the manufacturer's instructions (Beyotime, Shanghai, China).

2.3. Clinical samples

Ethical approval of this study was granted by the Huashan Institutional Review Board of Fudan University (HIRB). Three kidney tissue specimens were collected from patients with CaOx nephrolithiasis, and three paracancerous kidney tissue samples were obtained from patients who underwent radical nephrectomy of renal tumors as a control group. All subjects involved in the study provided informed consent.

2.4. Cell culture and treatment

The Human kidney 2 (HK-2) cell line was obtained from the Chinese Academy of Sciences (Shanghai, China), cultured at 37 °C in 5% CO_2 with DMEM/F12K culture medium (Gibco Technologies, Grand Island, USA) containing 10% fetal bovine serum (FBS) and 1% penicillin/streptomycin. Different levels of oxalate (0, 0.25, 0.5, 0.75, and 1 mM), sodium butyrate (NaB, 0, 0.05, 0.1, 0.5, and 1 mM) and Sulfaphenazole (SPZ, a specific CYP2C9 inhibitor, 10 μM) were treated into HK-2 for 24 h.

2.5. Cell counting Kit-8 (CCK-8) and lactate dehydrogenase (LDH) assay

The initial HK-2 cells were seeded equally (2×10^3) into 96-well plates after cell counting with trypan blue. After treatment with different levels of oxalic acid and butyrate, 10 μl of CCK-8 solution (Servicebio, Wuhan, China) was added at the designated time and the cell proliferation was then evaluated after 24h, 48h, 72h, and 96h at 450 nm absorbance with a Multiskan G0 (Thermo Fisher Scientific, Finland). Cellular LDH activities were determined with the LDH Assay Kit (Beyotime, Shanghai, China) following the manufacturer's instructions. Following centrifugation of the HK-2 cells, the released level of LDH in the supernatants was measured at 490 nm absorbance.

2.6. 4′-6-Diamidino-2-phenylindole (DAPI) staining assay

HK-2 cells were grown in 24-well glass slides and were exposed to different concentrations of oxalate and NaB. The cells in the wells were washed with phosphate-buffered saline (PBS), and then stained with DAPI (Absin, Shanghai, China) for 5 min and washed with PBS for 5 min twice, avoiding direct contact with light. Fluorescence images were detected by an inverted fluorescence microscope (TECAN, Switzerland).

2.7. Measurement of ROS levels

The 2,7-dichlorodihydrofuorescein diacetate (DCFH-DA) and Dihydroethidium (DHE) staining with microfluorimetry detection were used to determine ROS production. The Reactive Oxygen Species Assay Kit (DCFH-DA staining, Cat.No.50101ES01, YEASEN, Shanghai, China) and Dihydroethidium (DHE staining, Cat.No.50102ES02, YEASEN, Shanghai, China) were applied in this study. For DCFH-DA staining, treated cells were incubated in a serum-free media containing 10 μM DCFH-DA at 37 °C for 30 min. Then, the cells were collected and washed twice with serum-free media to remove the extracellular DCFH-DA. For DHE fluorescence staining, kidney tissue oxidant species and HK-2 cells were measured, respectively. Firstly, the kidney tissue was cleansed with PBS before frozen sections (5 μm). Afterwards, the sections were incubated with a 10 μM DHE solution at 37 °C for 30 min. Finally, fluorescence was observed after sealed with anti-fluorescence quencher. As for the *in vitro* study, the treated cells were exposed to 10 μM DHE for 60 min at 37 °C. Next, an inverted fluorescence microscope was used to observe ROS production (TECAN, Switzerland). Malondialdehyde (MDA), glutathione peroxidase (GSH-Px), and superoxide dismutase (SOD) activities in HK-2 cells were quantified by MDA, GSH-Px, and SOD kits (JianCheng, Nanjing, China), respectively.

2.8. Quantitative Real-time PCR (qRT-PCR) assays

Total RNA was extracted using the RNA simple Total Kit following the protocol (Vazyme, Nanjing, China) and then reverse-transcribed into cDNA. Notably, in triplicate, qRT-PCR was performed with three independent experiments in the SYBR Green PCR system (Vazyme, Nanjing, China). The primer sequences used in this article are listed in Table S1.

2.9. Flow cytometry apoptosis assay

Flow cytometry analysis was performed to determine if apoptosis was responsible for the reduced viability of HK-2 cells with an Annexin V-Fluorescein Isothiocyanate (FITC) Apoptosis Detection kit (YEASEN, Shanghai, China), according to the manufacturer's protocol. In brief, following 24h treatment, HK-2 cells were digested with trypsin and were then washed twice with PBS. After resuspended in 500 μl binding buffer,

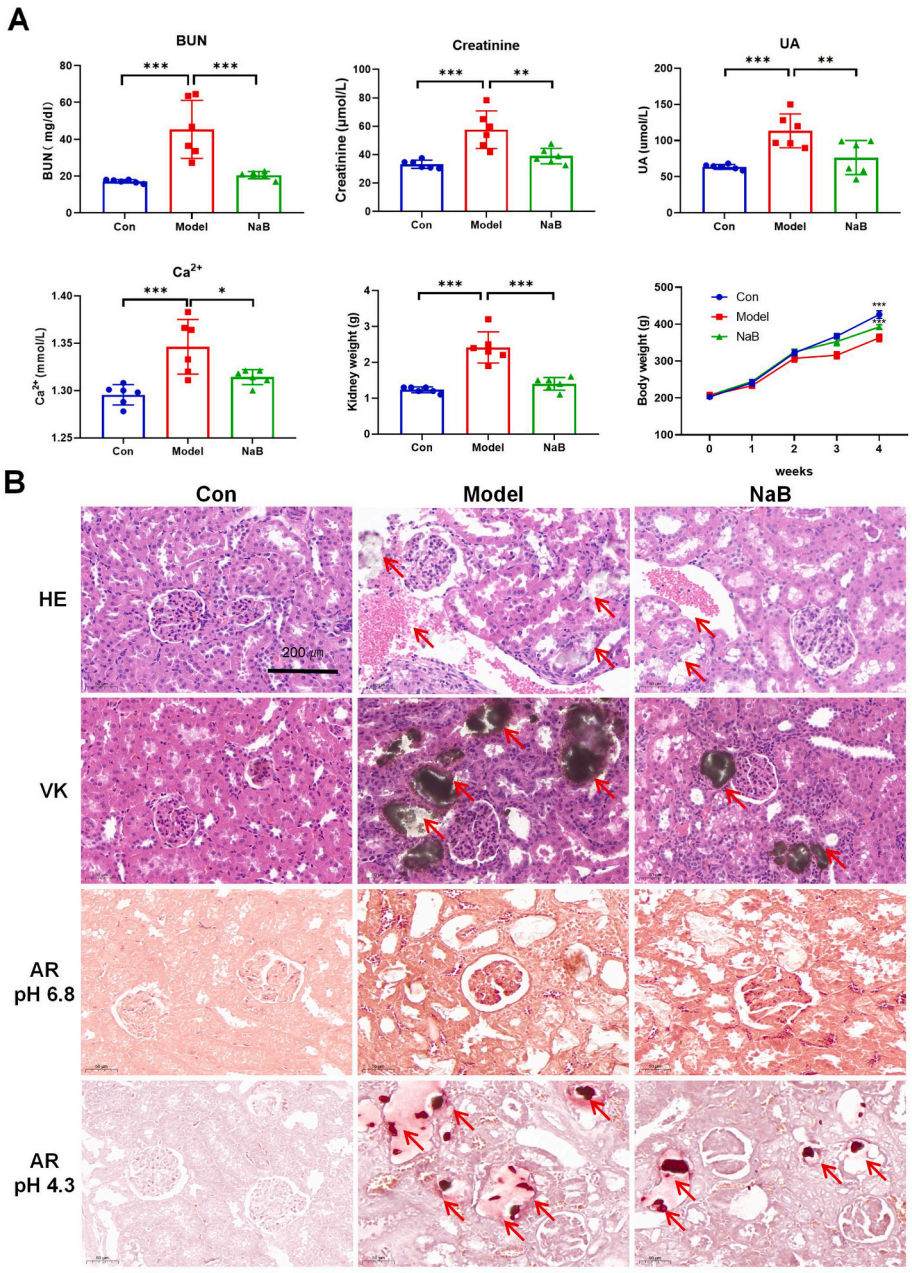

Fig. 1. Butyric acid reduced CaOx crystal deposition and kidney injury in rats. **(A)** Serum BUN, creatinine, UA, Ca^{2+}, kidney weight, and body weight of rats in the control, model, and NaB group (mean ± SD, n = 6, $^{*}P < 0.05$, $^{**}P < 0.01$, $^{***}P < 0.001$). **(B)** Pathological sections including HE, VK, and AR staining showed the degree of kidney injury and CaOx crystal deposition (magnification × 20; scale bar, 200 μm; arrows in H&E denote inflammation injury and crystal; arrows in VK denote calcium deposition; arrows in AR denote CaOx crystals).

followed by the addition of Annexin V-FITC (AV) and propidium iodide (PI) and subsequent mixing, HK-2 cells have incubated the reaction for 30 min at room temperature, protect from light. Finally, the cells were assessed by flow cytometry (Becton Dickinson, USA). The apoptotic cell rate was equal to the sum of the late apoptotic rate (upper right quadrant-advanced stage apoptosis cell percentage) and the early apoptotic rate (lower right quadrant-prophase apoptosis cell percentage).

2.10. Target genes prediction of butyric acid

The molecular structures of butyric acid and NaB were obtained from Pub-Chem (https://pubchem.ncbi.nlm.nih.gov/). Then, the SDF files of the 3D structure of butyric acid and NaB were uploaded to PharmMapper drug target screening database (http://lilab.ecust.edu.cn/pharmmapper/), to determine the predictive human protein targets related to the butyric acid and NaB. Finally, with UniProt database (https://www.uniprot.org/), the predicted protein lists were converted into the corresponding gene symbols. Thus, a total of 118 target genes of butyric acid were selected.

2.11. Protein-protein interaction (PPI) network and functional enrichment analysis

PPI network of the target genes was analyzed with STRING (https://www.string-db.org/) and an interaction score >0.7 was set as the threshold value. Then, Cytoscape 3.9.0 was used to analyze and visualize the hub genes, which were defined as genes that were highly interconnected with nodes in a module. In this experiment, the top 20 genes ranked with degrees were considered hub genes. Gene Ontology (GO) and Kyoto Encyclopedia of Genes and Genomes (KEGG) analyses were applied to explore possible biological processes (BPs) and molecular functions (MFs) and cellular components (CCs) of the target genes. The above analysis was performed by clusterProfiler," and "enrichplot" R packages. The first 5 enrichment results with $P < 0.05$ were visualized as a bubble diagram.

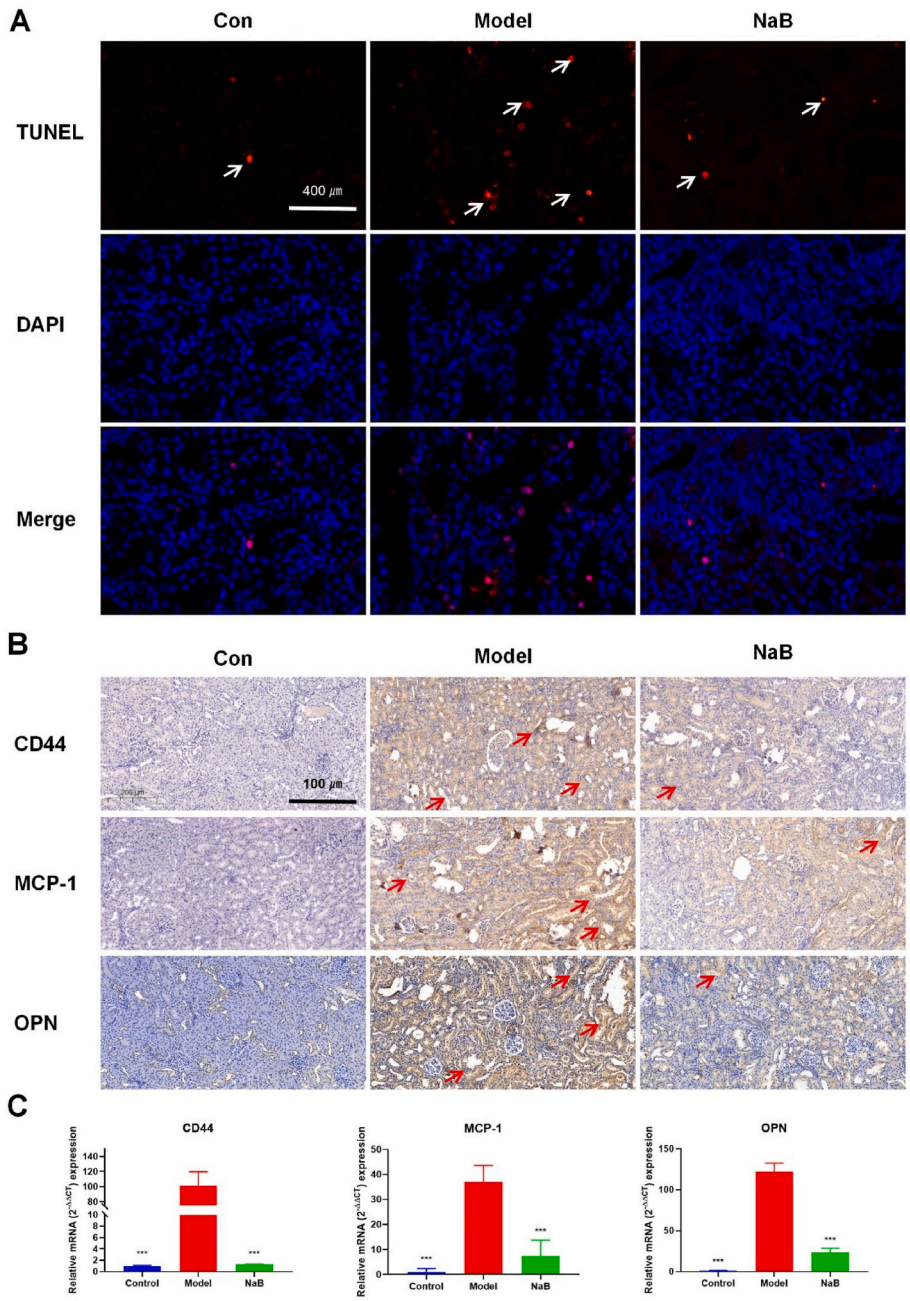

Fig. 2. Butyric acid ameliorated CaOx-induced apoptosis and inflammation injury in rats. (**A**) The TUNEL assay was performed to detect apoptotic cells (magnifcation × 40; scale bar, 400 μm; arrows denote apoptotic cells). (**B**) IHC analyses of CD44, MCP-1, and OPN proteins expression in renal tissues (magnifcation × 10; scale bar, 100 μm). (**C**) qRT-PCR analyses of CD44, MCP-1, and OPN mRNA expression in renal tissues. Data are presented as the mean values for each group (mean ± SD, n = 6, $^{***}P < 0.001$ vs. Model).

2.12. Differential genes analyses in GEO

The mRNA expression profile dataset of GSE73680 was downloaded from GEO (http://www.ncbi.nlm.nih.gov/geo/). GSE73680 is in GPL17077 platform (Agilent-039494 SurePrint G3 Human GE v2 8 × 60K Microarray 039381). This study contained 6 normal papillary tissue from control patients without any kidney stones as the control group (Con), and 26 Randall's Plaque tissues from calcium stone former as the experimental group (CaOx). With "limma" R package, genes with P value < 0.05 and absolute fold-change value > 1 were considered as differentially expressed genes (DEGs). The gene volcano map was generated with "ggplot2" R package, and the top 10 genes with the most significant up and downregulation were selected to draw the heat map with "heatmap" R package.

2.13. Potential targets of butyric acid against CaOx kidney stones

CaOx nephrolithiasis targets were sourced from GeneCards (https://www.genecards.org/). The keywords "calcium oxalate stones" and "calcium oxalate nephrolithiasis" were searched in GeneCards to acquire CaOx nephrolithiasis targets; then, a total of 370 CaOx nephrolithiasis target genes were selected. The Venn diagram displayed the common gene shared in PharmMapper, GEO, and GeneCards; thus, CYP2C9, the potential target gene of butyric acid against CaOx kidney stones, was selected. The network pharmacology analysis was performed by Bioprofifile (Shanghai, China).

2.14. Molecular docking

The high-resolution 3D chemical structure of CYP2C9 protein with the species configured with "Homosapiens" was downloaded from the Protein Data Bank (PDB, https://www.rcsb.org/) as a PDB file. The PDB

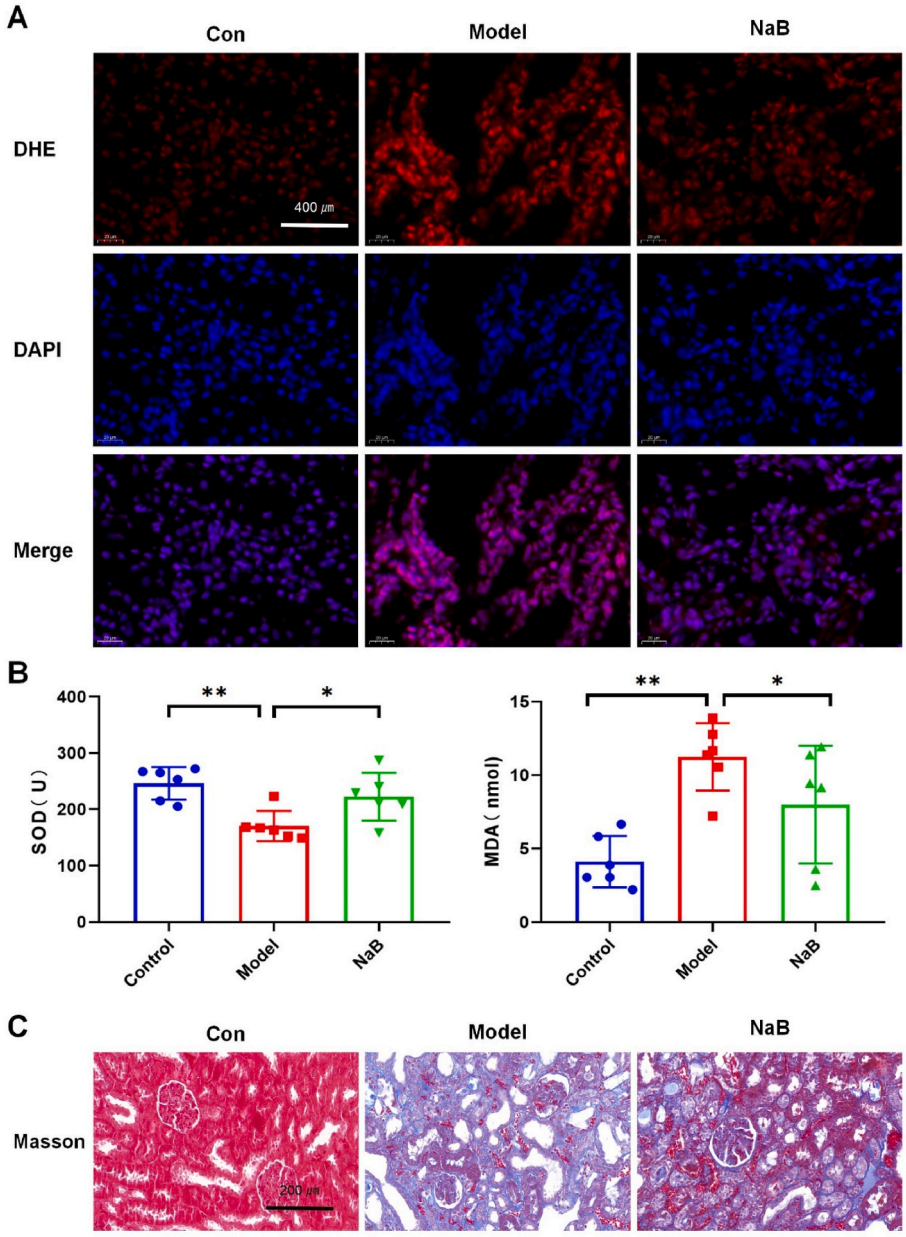

Fig. 3. Butyric acid reduced CaOx-induced oxidative stress in rats. **(A)** DHE staining was used to assess the cytoplasmic ROS generation in renal tissues (magnification × 40; scale bar, 400 μm). **(B)** SOD and MDA activities were detected in the control, model, and NaB group (mean ± SD, n = 6, $^{*}P < 0.05$, $^{**}P < 0.01$). **(C)** Masson staining revealed different degrees of fibrosis in different groups (magnification × 20; scale bar, 200 μm).

file of the treated receptor and ligand was imported into AutoDockTools (version 1.5.6) for routine processing and saved as the format file of PDBQT. Molecular docking was performed after butyric acid was chosen as the ligand. AutoDock Vina (version 1.1.2)71 was used in this project to conduct molecular docking for all calculations. Structure visualization was performed using PyMOL (http://www.pymol.org).

2.15. Statistical analysis

R software (version 4.0.1), SPSS (version 26.0) and GraphPad Prism (version 8.0) were utilized to perform the statistical analysis. The rational statistical test was employed to compare two independent test series (Student's t-test) or more test series (ANOVA test). A two-sided $P < 0.05$ indicated statistically significant.

3. Results

3.1. Butyric acid reduced formation of renal CaOx crystals and kidney injury in CaOx model rats

To investigate the effects of butyric acid on EG-induced kidney injury and CaOx crystal deposition, rat renal function and histopathological changes were detected. The results show that serum levels of creatinine, BUN, UA and Ca^{2+} in the CaOx model group were significantly higher than in the control group. Compared with the model group, NaB group serum levels of creatinine decreased by 32.2% (from 57.58 ± 13.22 to 39.03 ± 5.43 μmol/L), BUN decreased by 54.7% (from 45.33 ± 15.78 to 20.52 ± 1.96 mg/dl), UA decreased by 32.6% (from 113.4 ± 23.36 to 76.43 ± 23.58 μmol/L) and Ca^{2+} decreased by 2.37% (from 1.346 ± 0.029 to 1.314 ± 0.009 mmol/L), respectively, (Fig. 1A). In addition, the kidney weight notably increased while the body weight of rats in the

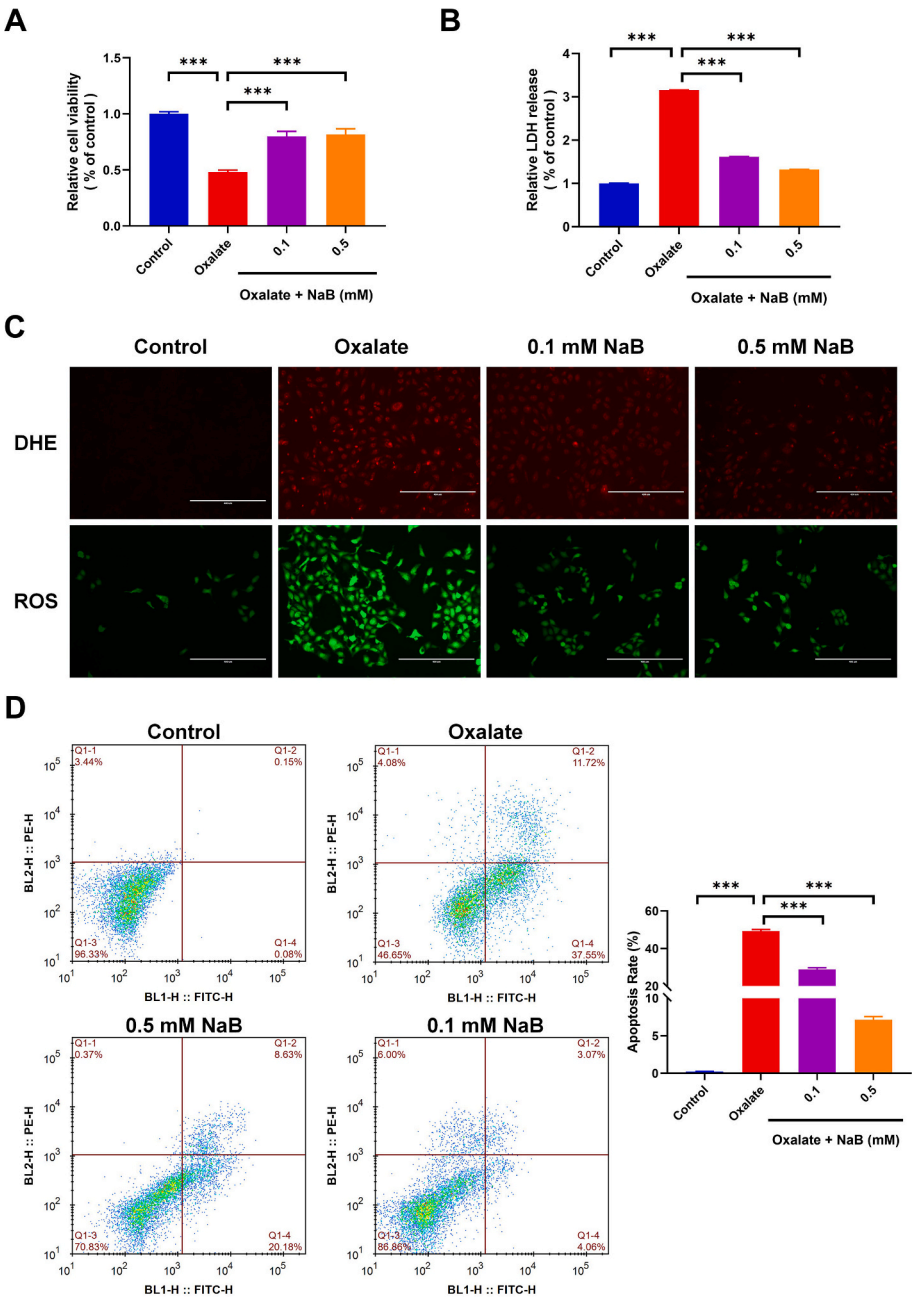

Fig. 4. Butyric acid suppressed oxalate-induced cytotoxicity, oxidative stress, and apoptosis in HK-2 cells. (**A-B)** Cell viability (A) and LDH release (B) after treatment with oxalate and/or NaB (mean ± SD, n = 3, ***$P < 0.001$). **(C)** DHE and ROS staining were used to assess the effect of NaB on cytoplasmic ROS generation in HK-2 cells (magnification × 40; scale bar, 400 μm). **(D)** Apoptotic rate of HK-2 cells was determined by flow cytometry (mean ± SD, n = 3, ***$P < 0.001$).

model group decreased significantly (Fig. 1A). HE, VK, and AR staining revealed the presence of CaOx crystals rather than calcium phosphate (CaP) crystals in the lumen of the renal tubules with tubular dilation in model rats; however, the administration of NaB was found to reduce the CaOx-induced kidney injury, which was characterized by the renal crystals and the abnormality of renal histologic structure such as tubular dilatation and loss of brush border (Fig. 1B). These findings demonstrated that butyric acid treatment significantly reduced EG-induced kidney injury and CaOx crystals.

3.2. Butyric acid ameliorated inflammation injury and oxidant species overexpression in CaOx model rats

TUNEL assay in conjunction with DAPI staining showed that the characteristic nuclear changes significantly occurred in the CaOx model group, including DNA cleavage, nuclear fragmentation (formation of apoptotic bodies), and nuclear shrinkage. The ameliorative effect of NaB on CaOx-mediated apoptosis damage was evaluated through TUNEL assay in rats' kidneys (Fig. 2A). IHC and qRT-PCR analysis showed that inflammatory injury markers OPN, MCP-1 and CD44 expression intensities were upregulated in the tubules in the CaOx model group compared with those in the control group while butyrate administration significantly inhibited MCP-1, CD44 and OPN protein expression in the NaB group (Fig. 2B–C).

The intensity of DHE fluorescence, ROS-sensitive fluorescent dye, increased in the CaOx model group, but NaB relieved the ROS level (Fig. 3A). To evaluate the role of NaB in oxidant stress further, SOD and MDA were measured to assess the level of lipid peroxidation in rat

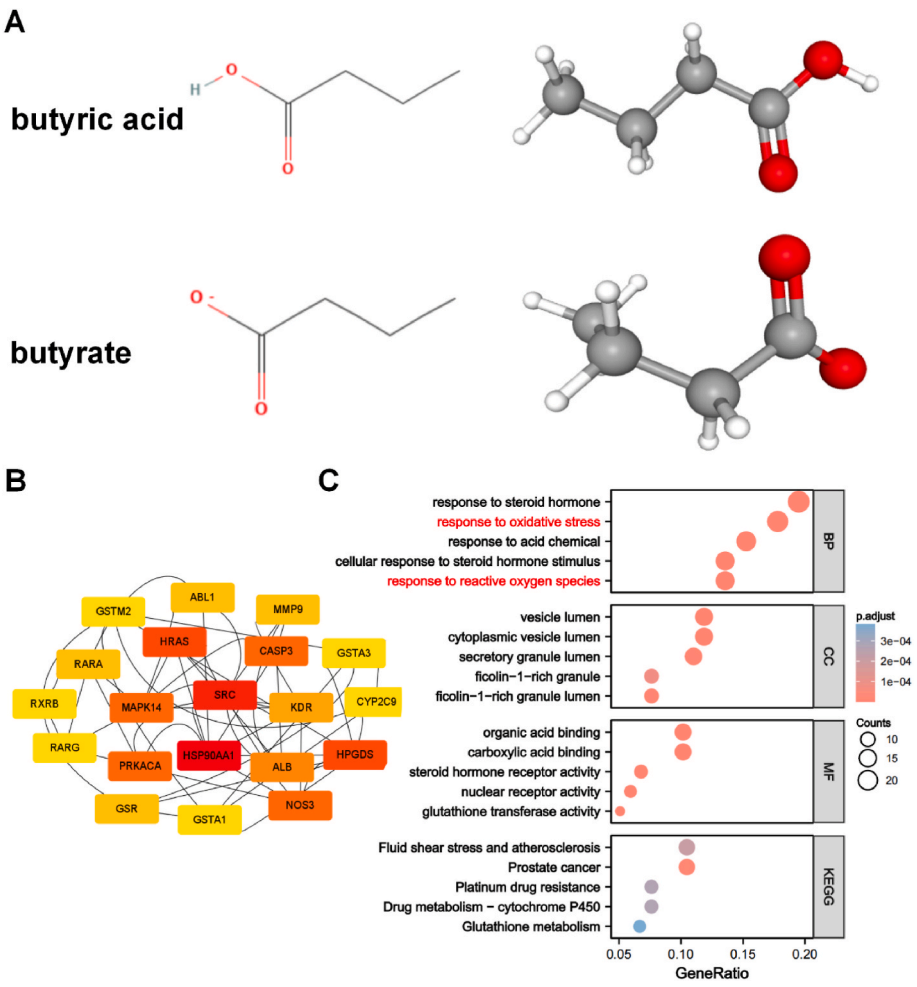

Fig. 5. Structure of butyric acid and target genes network analysis. **(A)** Two-dimensional and three-dimensional molecular structure of butyric acid and sodium butyrate. **(B)** Construction of the PPI network and hub genes were identified via PharmMapper database. **(C)** GO and KEGG enrichment pathways among hub genes.

kidneys. As illustrated in Fig. 3B, the SOD levels were significantly higher in the control and the NaB treatment group compared to the model group, whereas the MDA level demonstrated the opposite effect in the respective groups. Masson staining of renal samples showed that the control group had no renal interstitial fibrosis, while renal interstitial fibrosis was highlighted in the CaOx model group, which was improved after the NaB treatment (Fig. 3C).

3.3. Butyric acid suppressed oxalate-induced cell damage, oxidative stress, and apoptosis in HK-2 cells

With the CCK-8 assay, our data demonstrated that oxalic acid significantly decreased HK-2 cells' proliferation ability, which was concentration-dependent as well as time-dependent (Figs. S1A–B). Similarly, the oxalate treatment significantly increased LDH release in HK-2 cells in a time- and concentration-dependent manner (Figs. S1C–D). DAPI staining displayed condensed nuclei and apoptotic bodies in the oxalate group (Fig. S1E).

We selected 1 mM oxalic acid to treat HK-2 cells since significant cell injury was observed at this concentration. Then we first used different concentrations (0, 0.05, 0.1, 0.5, and 1 mM) of NaB to stimulate HK-2 cells (Fig. S1F). CCK-8 and LDH assays showed the cytoprotective effect of butyrate against renal injury caused by oxalic acid (Fig. 4A–B). Subsequently, we detected the generation of ROS using the ROS-sensitive fluorescent dye, DCFH-DA and DHE. The intensity of DCFH -DA and DHE fluorescence increased in the oxalate group, but was relieved after NaB treatment (Fig. 4C). The flow cytometry assays demonstrated that oxalate noticeably augmented the apoptosis of HK-2 cells; on the other hand, NaB inhibited the oxalate-induced apoptosis (Fig. 4D). These data suggested the cytoprotective potential of butyric acid against oxalate-induced injury in human renal epithelial cells.

3.4. Structure of butyric acid and target genes network analysis

The 2D and 3D structures of butyric acid and butyrate downloaded were obtained from PubChem (Fig. 5A). Then, the 3D structures were sent into PharmMapper database to get the human protein targets of butyric acid. Utilizing Uniprot database, we transformed the protein name into the relevant gene symbol. Finally, a total of 118 target genes of butyric acid were selected for further analysis. Next, the gene list was sent into STRING database to perform a PPI network (Fig. S2). The Cytoscape gave a detailed network diagram within the top 20 hub target genes ranked as degrees, including CYP2C9, CASP3, MAPK14, ALB, HRAS, ABL, RARA, RARG, RXRB, PRKACA, NOS3, SRC, MMP9, KDR, HSP90AA1, HPGDS, GSTA3, GSTA1, GSR, and GSTM2 (Fig. 5B). All these hub genes showed a certain correlation with other genes in the network, revealing that these genes may exert a cooperated function.

3.5. GO and KEGG enrichment analysis

GO and KEGG analyses uncovered the involved pathways and biological functions of the hub genes of butyric acid (Fig. 5C). According to the gene function classification of BP, the hub genes were mainly related to response to steroid hormone, response to oxidative stress, response to

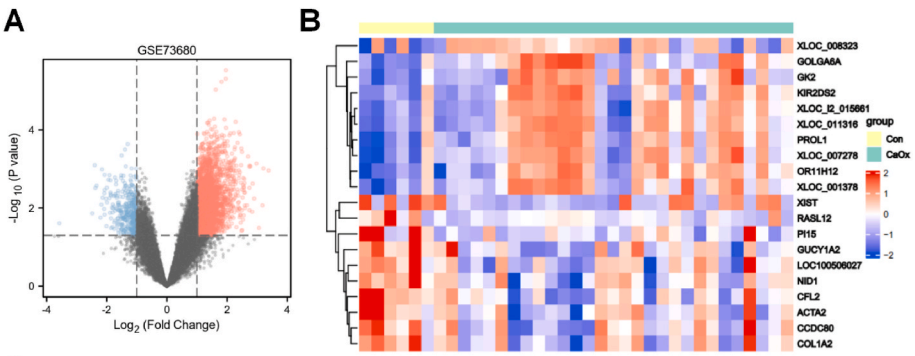

C

Gene Symbol	Description	Relevance score
CASR	Calcium Sensing Receptor	96.26260376
SLC26A1	Solute Carrier Family 26 Member 1	90.72318268
AGXT	Alanine--Glyoxylate And Serine--Pyruvate Aminotransferase	82.03861237
CLCN5	Chloride Voltage-Gated Channel 5	75.74562836
GRHPR	Glyoxylate And Hydroxypyruvate Reductase	70.93536377
SLC34A1	Solute Carrier Family 34 Member 1	70.25131226
VDR	Vitamin D Receptor	47.19543457
HOGA1	4-Hydroxy-2-Oxoglutarate Aldolase 1	46.44676208
SPP1	Secreted Phosphoprotein 1	44.77108383
ORAI1	ORAI Calcium Release-Activated Calcium Modulator 1	41.52308655

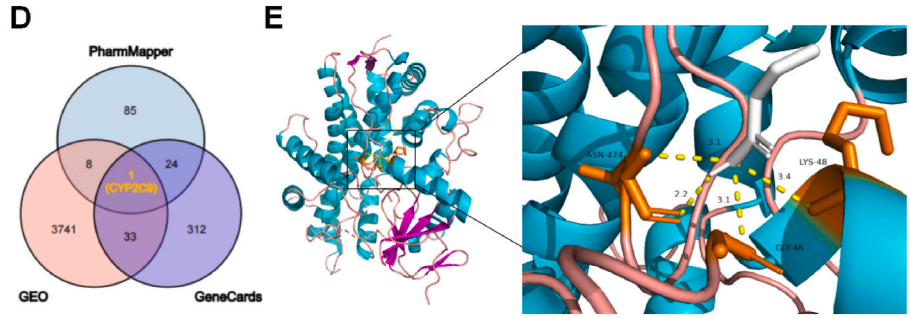

Fig. 6. CYP2C9 was the target gene of butyric acid on CaOx stones across multiple databases analysis. **(A)** Volcano plot of differentially expressed genes between CaOx stone patients and control in GEO. **(B)** Heat map of the top 20 differentially expressed genes between CaOx stone patients and control in GEO. **(C)** The top 10 CaOx stone-related genes were screened out from GeneCards database. **(D)** Venn diagram was acquired by taking the intersection of the targets of butyric acid in PharmMapper, the DEGs of nephrolithiasis in GEO, and the CaOx stones associated genes in GeneCards to find the key target gene (CYP2C9) of butyric acid on CaOx kidney stones. **(E)** Schematic diagram of butyric acid docking with CYP2C9.

reactive oxygen species, cellular response to steroid hormone stimulus, and response to acid chemical. Notably, butyric acid hub genes were gathered in metabolism-related processes like drug metabolism-cytochrome P450, platinum drug resistance, and glutathione metabolism. Remarkably, as mentioned above, these hub genes were involved in oxidative stress, and response to reactive oxygen species biological process, which were the vitally significant pathways of kidney stones formation mechanism, indicating that butyric acid might play a role in nephrolithiasis.

3.6. Target prediction of butyric acid on CaOx stones

Butyric acid acts as a natural inhibitor of histone deacetylase (HDACs), and meanwhile, it is reported that HDAC inhibitors may have therapeutic potential for the treatment of kidney stones (Wang et al., 2015). Similarly, depleted HDAC3 attenuates hyperuricemia-induced renal interstitial fibrosis (Hu et al., 2022). Hence, we explored the expression of HDACs in our animal models and cell models by RT-qPCR. The results showed that the expressions of HDACs were significantly elevated in the CaOx rat models and the oxalate-induced cell models (Fig. S3), but were alleviated by NaB treatment. Therefore, the effect of butyric acid on calcium oxalate-induced events could possibly be due to the inhibition of HDACs, but further research is still needed.

To further explore the exact target genes of butyric acid on CaOx nephrolithiasis, we first explored the DEGs between healthy control and CaOx stone patients in GSE73680 with GEO database. The screening criteria for significant DEGs were $P < 0.05$ and $|\log2(FC)| > 1$ between control and CaOx stone patients. The scatter plot of the DEGs is shown in Fig. 6A. After selection, a total of 3783 genes changed significantly, of which 3379 (89.4%) genes were upregulated, 404 (10.6%) genes were downregulated expression. Later, we performed the cluster analysis of DEGs and the heatmap presented the two-dimensional hierarchical clustering feature of the top 10 selected DEPs (Fig. 6B).

Subsequently, with GeneCards database, we manually identified 370 genes potentially related to CaOx nephrolithiasis. The top 20 predicted genes and their relevance scores were shown in Fig. 6C. Remarkably, to find the key target of butyric acid on CaOx kidney stones, a Venn diagram was acquired by taking the intersection of the targets of butyric acid in PharmMapper, the DEGs nephrolithiasis of in GEO, and the CaOx stones associated genes in GeneCards. Ultimately, CYP2C9 was identified as the potential target of butyric acid impacting on CaOx nephrolithiasis (Fig. 6D). Moreover, we performed the molecular docking of butyric acid and CYP2C9. Three amino acid residues, namely ASN-474, LYS-48, and GLY-46, of CYP2C9 interacted with quercetin with a hydrogen bonding energy of −4.2 kcal/mol, as illustrated in Fig. 6E.

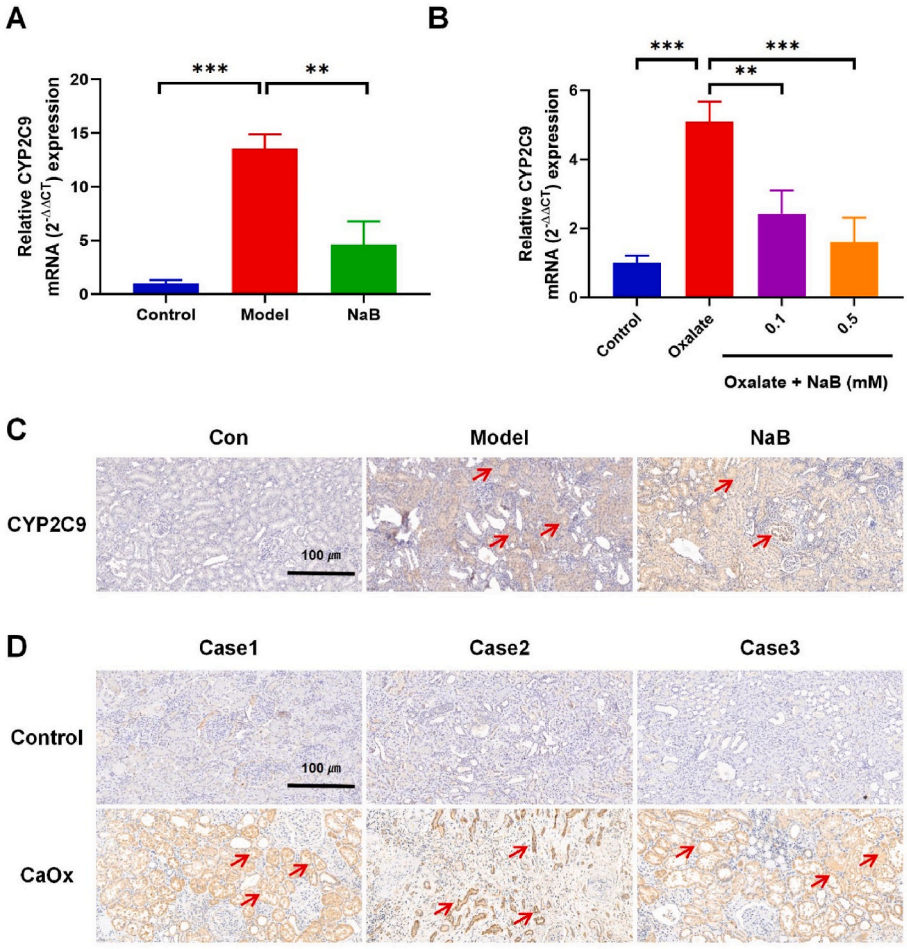

Fig. 7. CYP2C9 expression in CaOx rats, HK-2 cells and clinical samples. **(A-B)** qRT-PCR assays showed CYP2C9 expression in the kidney tissues of rats (A) and HK-2 cells (B) in each group (mean ± SD, n = 3, $^{**}P < 0.01$, $^{***}P < 0.001$). **(C)** IHC assays showed CYP2C9 expression in the kidney tissues of rats in each group (magnifcation × 10; scale bar, 100 μm). **(D)** IHC assays showed CYP2C9 expression in kidney tissues of clinical samples in each group (magnifcation × 10; scale bar, 100 μm).

3.7. Validation of target gene (CYP2C9) in CaOx rats, HK-2 cells, and clinical samples

Firstly, qRT-PCR results revealed that CYP2C9 mRNA expression increased compared with the control group, but decreased notably after NaB treatment in the CaOx rat model (Fig. 7A) and in HK-2 cells (Fig. 7B). Secondly, IHC assays confirmed this result in the CaOx rat model (Fig. 7C). Finally, compared with non-stone patients, CYP2C9 protein expression was elevated in CaOx stone patients via IHC analysis (Fig. 7D). These data strongly suggested that CYP2C9 was a potential target in CaOx nephrolithiasis.

3.8. Function of CYP2C9 in oxalate-induced HK-2 cells

Furthermore, we explored CYP2C9 function in HK-2 cell injury model with Sulfaphenazole (SPZ), a specific inhibitor of CYP2C9. qRT-PCR assays showed CYP2C9 expression significantly downregulated in HK-2 cells when exposed to SPZ and NaB (Fig. 8A). After suppressing CYP2C9 by SPZ and NaB, the oxalate-induced cell growth inhibition and LDH release were markedly ameliorated (Fig. 8B–C). DCFH-DA and DHE fluorescence was measured to determine the total intracellular oxidant species level. Treatment with SPZ significantly decreased intracellular oxidant species and mitochondrial oxidant species generation compared with oxalate-induced cells (Fig. 8D). To gain a better understanding of CYP2C9's role in oxidant stress, SOD and MDA levels were assessed. As illustrated in Fig. 8E, the SOD and GSH-Px levels were markedly increased in the SPZ and NaB treatment group when compared to the oxalate group, while the MDA level revealed contrasting effects.

In addition, the inhibition of CYP2C9 by SPZ and NaB resulted in apoptosis suppression in HK-2 cell injury model (Fig. 9A). Also, we screened and examined the levels of apoptosis-related proteins in HK-2 injury cell model. qRT-PCR assays reflected that oxalate stimulation significantly increased the expression of proapoptotic proteins Cleaved Caspase-3 and Bax, while reduced antiapoptotic proteins Bcl-2 expression, which was alleviated by SPZ and NaB (Fig. 9B). In addition, the fold change in mRNA levels of HK-2 cells due to oxalate exposure was significantly increased in inflammation injury biomarkers, including CD44, MCP-1, and OPN, compared to the untreated controls, but were drastically reduced after cotreated with SPZ and NaB (Fig. 9C). Collectively, CYP2C9 has a major role in promoting oxidative stress and apoptosis damage.

4. Discussion

In this study, we explored the protective effect of butyrate on CaOx animal and cell models. Firstly, we confirmed that butyrate dramatically reversed 0.75% EG-induced CaOx crystal deposition in SD rats' kidneys by inhibiting oxidative stress and inflammation in tubular cells. It is currently believed that the formation of kidney stones in humans is caused by oxalate-induced damage to renal tubular epithelial cells, which leads to the accumulation of CaOx crystals and their subsequent adherence (Evan et al., 2015; Khan et al., 2016). Hence, the human renal tubular epithelial cells, HK-2 cells, were established to confirm the cytoprotective effects of butyric acid on CaOx stones in this research. With the cell model, we found the regulatory mechanism of butyrate in CaOx kidney-stone formation through its control of the CYP2C9/ROS pathway, inducing oxidative stress by disrupting ROS levels and accompanying modulation of inflammation and apoptosis.

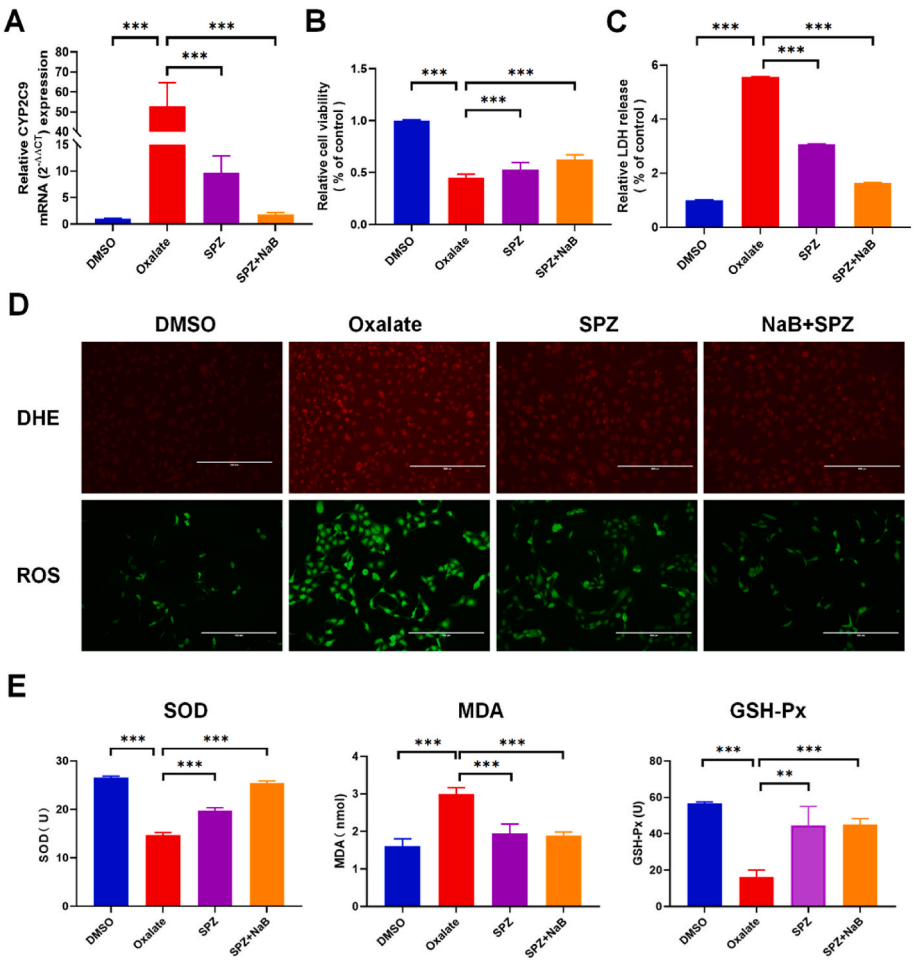

Fig. 8. Function of CYP2C9 in oxalate-induced HK-2 cells. **(A)** qRT-PCR assays showed CYP2C9 expression in HK-2 oxalate model with or without SPZ/NaB (mean ± SD, n = 3, ***$P < 0.001$). **(B–C)** Cell viability (B) and LDH release (C) in HK-2 oxalate model with or without SPZ/NaB (mean ± SD, n = 3, ***$P < 0.001$). **(D)** DHE and ROS staining were used to assess the effect of SPZ and NaB on cytoplasmic ROS generation in HK-2 oxalate model (magnification × 40; scale bar, 400 μm). **(E)** SOD, MDA, and GSH-Px activity were detected in HK-2 oxalate model with or without SPZ/NaB (mean ± SD, n = 3, **$P < 0.01$, ***$P < 0.001$).

Butyric acid, as an important SCFA, was derived from the metabolism of intestinal bacteria (Liu et al., 2018). Numerous studies have underlined the advantages of butyric acid in regulating host metabolism, inflammation, and immunity (Lanza et al., 2022; Okumura et al., 2021; Wang et al., 2022). For example, butyrate depletion and its repletion appear to play a central role in necrotising pancreatitis (van den Berg et al., 2021). Xu et al. reported that NaB intervention could improve intestinal barrier function and inflammation in diabetic mice via regulating the intestinal microflora structure (Xu et al., 2018). In chronic kidney disease, Li and others uncovered a novel beneficial role of butyrate-mediated GPR-43 signaling in the restoration of renal function (Li et al., 2022a). Notably, a recent study has shown that SCFAs including butyric acid could reduce CaOx stones by regulating intestinal oxalate transporter SLC26A6 *in vivo* (Liu et al., 2021). However, the specific potential targets of butyric acid on CaOx stones have not been explored in depth. Therefore, we predicted the butyric acid target genes on CaOx nephrolithiasis with network pharmacology and validated the function of the target gene CYP2C9. As reported, oxalate-induced nephrolithiasis primarily occurs through renal tubular epithelial cell damage (Liu et al., 2022; Peng et al., 2019). Consistently, our study revealed that butyrate effectively protected renal cells from oxalate injury, including increased cell viability and decreased LDH release. Additionally, the effects of butyrate on oxidative stress factors were observed to explore its intervention and possible mechanism of renal CaOx stones formation. Elucidating the relationship and mechanism between butyric acid and CaOx stones holds great importance for treating and preventing this condition.

Network pharmacology analysis indicated that CYP2C9 was the target gene of butyric acid on CaOx stones. CYPs are pivotal in drug detoxification and can stimulate mono-oxygenation and detoxification reactions accompanied by a significant production of toxic ROS (Gómez-Tabales et al., 2020). Furthermore, CYP450s are vital for keeping the normal physiological operation of the kidney (Hao and Breyer, 2007). Among CYPs family, CYP2C9 is involved in the metabolic and transformational processes of a host of endogenous substances (Sangkuhl et al., 2021). Moreover, CYP2C9 is emerging as a pivotal regulator of oxidative stress involved in ROS production and the CYP2C9/ROS pathway has an essential role in regulating cell apoptosis (Zhang et al., 2018). In line with this view, we found that the CYP2C9 mRNA levels and ROS levels in the CaOx group were increased compared to the control group. Besides, our results revealed that CYP2C9 expression was dramatically reduced under butyric acid treatment, which manifested that CYP2C9 may be a potential target of butyrate in renal tubular epithelial cells. SPZ is a special inhibitor of CYP2C9 which was used to explore the function of CYP2C9 in CaOx stones in our research. Then, we found that SPZ treatment in the oxalate exposure group could notably enhance HK-2 cells activity, but decrease CYP2C9 and ROS levels, and ultimately suppress inflammation and apoptosis levels, suggesting that CYP2C9 might play an important role in CaOx stones. Notably, network pharmacology results also indicated that extracellular calcium-sensing receptor (CASR) could be interestingly shown as a gene involve in stone formation. CASR, a dimeric G protein-coupled receptor, is involved in the regulation of parathyroid hormone release and Ca2+ homeostasis (Riccardi and Valenti, 2016). In our previous study conducted in the Chinese Han population, polymorphisms of CASR-related genes (WDR72, DGKH, and CLDN14) were associated with increased susceptibility to calcium nephrolithiasis (Li et al., 2022b), in accordance with a prior study by Howles et al. (2019).

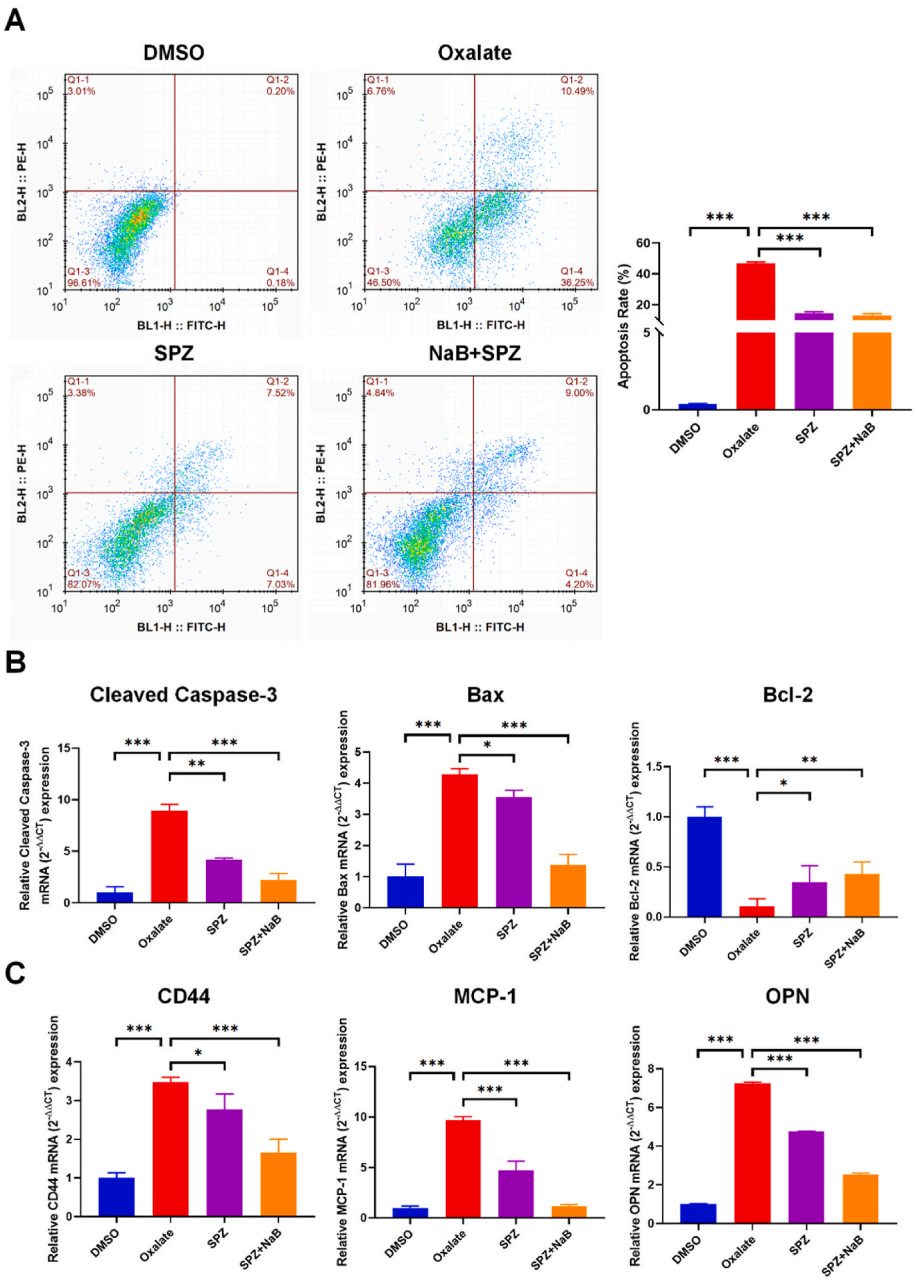

Fig. 9. Inhibition of CYP2C9 resulted in apoptosis suppression in HK-2 cells. **(A)** Apoptotic rate of HK-2 cells was determined by flow cytometry (mean ± SD, n = 3, ***$P < 0.001$). **(B–C)** Levels of Cleaved Caspase-3, Bcl-2, Bax (B), OPN, CD44, and MCP-1 (C) mRNA in HK-2 oxalate model with or without SPZ/NaB (mean ± SD, n = 3, *$P < 0.05$, **$P < 0.01$, ***$P < 0.001$).

It has been suggested that CASR activation at the cell surface is a key factor in the formation of calcium-containing stones, since it reduces the abundance of aquaporin-2 in the membrane, thus limiting water conservation and providing protection against the formation of stones (Renkema et al., 2011). Nevertheless, some studies have presented conflicting evidence regarding the role of CASR in nephrolithiasis. For instance, Ibeh et al. found that CASR existed in the proximal tubule, mediated transcellular Ca2+ transport and mitigated the formation of the calcium crystals (Ibeh et al., 2019). Further research is needed to better understand the molecular mechanisms of CASR in nephrolithiasis.

ROS, a product generated in the process of oxidation, is involved in the emergence of several ailments (Zorov et al., 2014). It is currently accepted that ROS is a trigger and regulator of apoptosis and inflammation, leading to tubular damage, as well as the attachment and accumulation of crystals (Lu et al., 2021). Recently, Joshi et al. found that the tubular epitheliums exposure to CaOx crystals induces the production of ROS with the involvement of NADPH oxidase in CaOx stones formation (Joshi and Khan, 2019). Similarly, our findings demonstrated that butyric acid could ameliorate inflammation injury and oxidant species overexpression in the CaOx animal model. Consistently, our results showed that oxalate exposure could induce the overproduction of ROS in HK-2 cells. However, under butyric acid and/or SPZ treatment, data manifested that ROS, inflammation, and apoptosis levels were markedly decreased, revealing that butyric acid and CYP2C9 may exert their roles primarily through signaling pathways linking oxidative stress to apoptosis.

Attention is growing for the utilization of butyric acid, one of the most efficient natural beneficial gut metabolites, due to the minimal amounts of unfavorable reactions it causes (Hsu et al., 2022; Morris et al., 2017). Butyric acid has been shown to protect against oxidative

stress and inflammation response in human diseases (Liang et al., 2013; Liu et al., 2017; Zhou et al., 2022). For example, Hu and others found that butyrate and acetate could improve β-cell metabolism and mitochondrial respiration under oxidative stress (Hu et al., 2020). Tang et al. exemplified that NaB protects against oxidative stress in high-fat-diet-induced obese rats by promoting mitochondrial function (Tang et al., 2022). However, in some studies, butyric acid has been shown to induce the production of ROS in certain cell lines or experimental models. Research has demonstrated that butyric acid at higher concentrations might promote ROS generation in immune cells like T cells (Kurita-Ochiai et al., 2003; Kurita-Ochiai and Ochiai, 2010) and macrophages (Yang et al., 2019), colorectal cancer cells (Doublier et al., 2022; Wang et al., 2023), and human gingival fibroblasts (Chang et al., 2013). Therefore, while butyric acid generally possesses antioxidant properties, it can also induce ROS production in certain cellular contexts. The exact effects of butyric acid on ROS production can vary and may depend on the specific cell type and experimental conditions. Whereas, few studies have been conducted about the mechanism of butyric acid impacting the CaOx stone. Our research provides insight into the role and mechanism of butyric acid as well as CYP2C9 in CaOx nephrolithiasis. To the best of our knowledge, none of the previous urolithiasis studies has reported on the role of CYP2C9 in CaOx nephrolithiasis. This study may provide experimental evidence that CYP2C9/ROS may serve as the therapeutic targets in CaOx stones. In particular, the methods of preventing and treating kidney stones have been essentially the same for decades (Chen et al., 2015), making this discovery particularly important. New medical prophylaxis needs to be developed that is safe and effective, thus, research into the potential use of butyric acid as a prophylactic measure for those suffering from kidney stones is highly recommended.

It is important to recognize the limitations of this research: (1) The rat model is not capable of accurately replicating the development of CaOx nephrolithiasis, despite the fact that EG exposure through drinking water in Wistar or SD rats is a commonly used animal model for studying hyperoxaluria and CaOx nephrolithiasis; further studies involving different animal models of CaOx nephrolithiasis, larger sample sizes, and multiple centers involving patients are necessary to gain a more comprehensive understanding; (2) butyric acid is unstable, which may be impacted by other unidentifiable factors; (3) further drug toxicology evaluations and clinical trials are needed to confirm preventive and therapeutic effects of butyric acid; (4) It is better to have NaB alone group in animal experiment, which will make the study more rigorous and objective.

5. Conclusions

The present study indicated that butyric acid could rescue the inflammation and oxidative stress injury via targeting CYP2C9 in the CaOx nephrolithiasis model. Thus, butyric acid may have potential clinical applications that could help to prevent the occurrence of CaOx nephrolithiasis.

CRediT authorship contribution statement

Zijian Zhou: Formal analysis, Data curation, Conceptualization, Writing – original draft. **Xuan Zhou:** Data curation, Formal analysis. **Yu Zhang:** Formal analysis, Data curation. **Yuanyuan Yang:** Formal analysis. **Lujia Wang:** Funding acquisition, Writing – review & editing. **Zhong Wu:** Funding acquistion, Writing – review & editing.

Declaration of competing interest

The authors declare that they have no known competing financial interests or personal relationships that could have appeared to influence the work reported in this paper.

Data availability

Data will be made available on request.

Acknowledgements

This research was funded by the National Natural Science Foundation of China (No. 81970603 and No. 82100807).

Appendix A. Supplementary data

Supplementary data to this article can be found online at https://doi.org/10.1016/j.fct.2023.113925.

References

Awuah Boadi, E., Shin, S., Yeroushalmi, S., Choi, B.E., Li, P., Bandyopadhyay, B.C., 2021. Modulation of tubular pH by acetazolamide in a Ca(2+) transport deficient mice facilitates calcium nephrolithiasis. Int. J. Mol. Sci. 22.
Bayazid, A.B., Kim, J.G., Azam, S., Jeong, S.A., Kim, D.H., Park, C.W., Lim, B.O., 2022. Sodium butyrate ameliorates neurotoxicity and exerts anti-inflammatory effects in high fat diet-fed mice. Food Chem. Toxicol. : an international journal published for the British Industrial Biological Research Association 159, 112743.
Chang, M.C., Tsai, Y.L., Chen, Y.W., Chan, C.P., Huang, C.F., Lan, W.C., Lin, C.C., Lan, W. H., Jeng, J.H., 2013. Butyrate induces reactive oxygen species production and affects cell cycle progression in human gingival fibroblasts. J. Periodontal. Res. 48, 66–73.
Chen, T.T., Wang, C., Ferrandino, M.N., Scales, C.D., Yoshizumi, T.T., Preminger, G.M., Lipkin, M.E., 2015. Radiation exposure during the evaluation and management of nephrolithiasis. J. Urol. 194, 878–885.
Crivelli, J.J., Maalouf, N.M., Paiste, H.J., Wood, K.D., Hughes, A.E., Oates, G.R., Assimos, D.G., 2021. Disparities in kidney stone disease: a scoping review. J. Urol. 206, 517–525.
Danpure, C.J., Rumsby, G., 2004. Molecular aetiology of primary hyperoxaluria and its implications for clinical management. Expet Rev. Mol. Med. 6, 1–16.
Doublier, S., Cirrincione, S., Scardaci, R., Botta, C., Lamberti, C., Giuseppe, F.D., Angelucci, S., Rantsiou, K., Cocolin, L., Pessione, E., 2022. Putative probiotics decrease cell viability and enhance chemotherapy effectiveness in human cancer cells: role of butyrate and secreted proteins. Microbiol. Res. 260, 127012.
Evan, A.P., Worcester, E.M., Coe, F.L., Williams Jr., J., Lingeman, J.E., 2015. Mechanisms of human kidney stone formation. Urolithiasis 43 (Suppl. 1), 19–32.
Fakhoury, M.Q., Gordon, B., Shorter, B., Renson, A., Borofsky, M.S., Cohn, M.R., Cabezon, E., Wysock, J.S., Bjurlin, M.A., 2019. Perceptions of dietary factors promoting and preventing nephrolithiasis: a cross-sectional survey. World J. Urol. 37, 1723–1731.
Fukami, T., Yokoi, T., Nakajima, M., 2022. Non-P450 drug-metabolizing enzymes: contribution to drug disposition, toxicity, and development. Annu. Rev. Pharmacol. Toxicol. 62, 405–425.
Gómez-Tabales, J., García-Martín, E., Agúndez, J.A.G., Gutierrez-Merino, C., 2020. Modulation of CYP2C9 activity and hydrogen peroxide production by cytochrome b (5). Sci. Rep. 10, 15571.
Hao, C.M., Breyer, M.D., 2007. Physiologic and pathophysiologic roles of lipid mediators in the kidney. Kidney Int. 71, 1105–1115.
Howles, S.A., Wiberg, A., Goldsworthy, M., Bayliss, A.L., Gluck, A.K., Ng, M., Grout, E., Tanikawa, C., Kamatani, Y., Terao, C., Takahashi, A., Kubo, M., Matsuda, K., Thakker, R.V., Turney, B.W., Furniss, D., 2019. Genetic variants of calcium and vitamin D metabolism in kidney stone disease. Nat. Commun. 10, 5175.
Hsu, C.N., Yu, H.R., Lin, I.C., Tiao, M.M., Huang, L.T., Hou, C.Y., Chang-Chien, G.P., Lin, S., Tain, Y.L., 2022. Sodium butyrate modulates blood pressure and gut microbiota in maternal tryptophan-free diet-induced hypertension rat offspring. J. Nutr. Biochem. 108, 109090.
Hu, L., Yang, K., Mai, X., Wei, J., Ma, C., 2022. Depleted HDAC3 attenuates hyperuricemia-induced renal interstitial fibrosis via miR-19b-3p/SF3B3 axis. Cell Cycle 21, 450–461.
Hu, S., Kuwabara, R., de Haan, B.J., Smink, A.M., de Vos, P., 2020. Acetate and butyrate improve β-cell metabolism and mitochondrial respiration under oxidative stress. Int. J. Mol. Sci. 21.
Ibeh, C.L., Yiu, A.J., Kanaras, Y.L., Paal, E., Birnbaumer, L., Jose, P.A., Bandyopadhyay, B.C., 2019. Evidence for a regulated Ca(2+) entry in proximal tubular cells and its implication in calcium stone formation. J. Cell Sci. 132.
Joshi, S., Khan, S.R., 2019. Opportunities for future therapeutic interventions for hyperoxaluria: targeting oxidative stress. Expert Opin. Ther. Targets 23, 379–391.
Khan, S.R., 2013. Reactive oxygen species as the molecular modulators of calcium oxalate kidney stone formation: evidence from clinical and experimental investigations. J. Urol. 189, 803–811.
Khan, S.R., Pearle, M.S., Robertson, W.G., Gambaro, G., Canales, B.K., Doizi, S., Traxer, O., Tiselius, H.G., 2016. Kidney stones. Nat. Rev. Dis. Prim. 2, 16008.
Knoll, T., Schubert, A.B., Fahlenkamp, D., Leusmann, D.B., Wendt-Nordahl, G., Schubert, G., 2011. Urolithiasis through the ages: data on more than 200,000 urinary stone analyses. J. Urol. 185, 1304–1311.
Kurita-Ochiai, T., Amano, S., Fukushima, K., Ochiai, K., 2003. Cellular events involved in butyric acid-induced T cell apoptosis. J. Immunol. 171, 3576–3584.

Kurita-Ochiai, T., Ochiai, K., 2010. Butyric acid induces apoptosis via oxidative stress in Jurkat T-cells. J. Dent. Res. 89, 689–694.
Lanza, M., Scuderi, S.A., Filippone, A., Casili, G., Campolo, M., Paterniti, I., Cuzzocrea, S., Esposito, E., 2022. The role of SCFAs on microbiota composition in a mouse model of NTG-induced migraine. Faseb. J. 36 (Suppl. 1).
Li, H.B., Xu, M.L., Xu, X.D., Tang, Y.Y., Jiang, H.L., Li, L., Xia, W.J., Cui, N., Bai, J., Dai, Z.M., Han, B., Li, Y., Peng, B., Dong, Y.Y., Aryal, S., Manandhar, I., Eladawi, M. A., Shukla, R., Kang, Y.M., Joe, B., Yang, T., 2022a. Faecalibacterium prausnitzii attenuates CKD via butyrate-renal GPR43 Axis. Circ. Res. 131, e120–e134.
Li, Y., Huang, C., Yang, Z., Wang, L., Luo, D., Qi, L., Li, Z., Huang, Y., 2022b. Identification of potential biomarkers of gout through competitive endogenous RNA network analysis. Eur. J. Pharmaceut. Sci. : official journal of the European Federation for Pharmaceutical Sciences, 106180.
Liang, X., Wang, R.S., Wang, F., Liu, S., Guo, F., Sun, L., Wang, Y.J., Sun, Y.X., Chen, X.L., 2013. Sodium butyrate protects against severe burn-induced remote acute lung injury in rats. PLoS One 8, e68786.
Liu, H., Wang, J., He, T., Becker, S., Zhang, G., Li, D., Ma, X., 2018. Butyrate: a double-edged sword for health? Adv. Nutri. (Bethesda, Md.) 9, 21–29.
Liu, J., Fu, Y., Zhang, H., Wang, J., Zhu, J., Wang, Y., Guo, Y., Wang, G., Xu, T., Chu, M., Wang, F., 2017. The hepatoprotective effect of the probiotic Clostridium butyricum against carbon tetrachloride-induced acute liver damage in mice. Food Funct. 8, 4042–4052.
Liu, Y., Jin, X., Hong, H.G., Xiang, L., Jiang, Q., Ma, Y., Chen, Z., Cheng, L., Jian, Z., Wei, Z., Ai, J., Qi, S., Sun, Q., Li, H., Li, Y., Wang, K., 2020. The relationship between gut microbiota and short chain fatty acids in the renal calcium oxalate stones disease. Faseb. J. 34, 11200–11214.
Liu, Y., Jin, X., Ma, Y., Jian, Z., Wei, Z., Xiang, L., Sun, Q., Qi, S., Wang, K., Li, H., 2021. Short-Chain Fatty Acids Reduced Renal Calcium Oxalate Stones by Regulating the Expression of Intestinal Oxalate Transporter SLC26A6. mSystems, e0104521.
Liu, Y., Sun, Y., Kang, J., He, Z., Liu, Q., Wu, J., Li, D., Wang, X., Tao, Z., Guan, X., She, W., Xu, H., Deng, Y., 2022. Role of ROS-induced NLRP3 inflammasome activation in the formation of calcium oxalate nephrolithiasis. Front. Immunol. 13, 818625.
Lu, H., Sun, X., Jia, M., Sun, F., Zhu, J., Chen, X., Chen, K., Jiang, K., 2021. Rosiglitazone suppresses renal crystal deposition by ameliorating tubular injury resulted from oxidative stress and inflammatory response via promoting the Nrf2/HO-1 pathway and shifting macrophage polarization. Oxid. Med. Cell. Longev. 2021, 5527137.
Luzardo-Ocampo, I., Loarca-Piña, G., Gonzalez de Mejia, E., 2020. Gallic and butyric acids modulated NLRP3 inflammasome markers in a co-culture model of intestinal inflammation. Food Chem. Toxicol. : an international journal published for the British Industrial Biological Research Association 146, 111835.
Morris, G., Berk, M., Carvalho, A., Caso, J.R., Sanz, Y., Walder, K., Maes, M., 2017. The role of the microbial metabolites including tryptophan catabolites and short chain fatty acids in the pathophysiology of immune-inflammatory and neuroimmune disease. Mol. Neurobiol. 54, 4432–4451.
Okumura, S., Konishi, Y., Narukawa, M., Sugiura, Y., Yoshimoto, S., Arai, Y., Sato, S., Yoshida, Y., Tsuji, S., Uemura, K., Wakita, M., Matsudaira, T., Matsumoto, T., Kawamoto, S., Takahashi, A., Itatani, Y., Miki, H., Takamatsu, M., Obama, K., Takeuchi, K., Suematsu, M., Ohtani, N., Fukunaga, Y., Ueno, M., Sakai, Y., Nagayama, S., Hara, E., 2021. Gut bacteria identified in colorectal cancer patients promote tumourigenesis via butyrate secretion. Nat. Commun. 12, 5674.
Peng, Y., Fang, Z., Liu, M., Wang, Z., Li, L., Ming, S., Lu, C., Dong, H., Zhang, W., Wang, Q., Shen, R., Xie, F., Zhang, W., Yang, C., Gao, X., Sun, Y., 2019. Testosterone induces renal tubular epithelial cell death through the HIF-1α/BNIP3 pathway. J. Transl. Med. 17, 62.
Proia, A.D., Brinn, N.T., 1985. Identification of calcium oxalate crystals using alizarin red S stain. Arch. Pathol. Lab Med. 109, 186–189.
Renkema, K.Y., Bindels, R.J., Hoenderop, J.G., 2011. Role of the calcium-sensing receptor in reducing the risk for calcium stones. Clin. J. Am. Soc. Nephrol. : CJASN 6, 2076–2082.
Riccardi, D., Valenti, G., 2016. Localization and function of the renal calcium-sensing receptor. Nat. Rev. Nephrol. 12, 414–425.
Rysz, J., Franczyk, B., Kujawski, K., Sacewicz-Hofman, I., Ciałkowska-Rysz, A., Gluba-Brzózka, A., 2021. Are nutraceuticals beneficial in chronic kidney disease? Pharmaceutics 13.
Sangkuhl, K., Claudio-Campos, K., Cavallari, L.H., Agundez, J.A.G., Whirl-Carrillo, M., Duconge, J., Del Tredici, A.L., Wadelius, M., Rodrigues Botton, M., Woodahl, E.L., Scott, S.A., Klein, T.E., Pratt, V.M., Daly, A.K., Gaedigk, A., 2021. PharmVar GeneFocus: CYP2C9. Clin. Pharmacol. Ther. 110, 662–676.
Schulthess, J., Pandey, S., Capitani, M., Rue-Albrecht, K.C., Arnold, I., Franchini, F., Chomka, A., Ilott, N.E., Johnston, D.G.W., Pires, E., McCullagh, J., Sansom, S.N., Arancibia-Cárcamo, C.V., Uhlig, H.H., Powrie, F., 2019. The short chain fatty acid butyrate imprints an antimicrobial program in macrophages. Immunity 50, 432–445 e437.
Shin, S., Ibeh, C.L., Awuah Boadi, E., Choi, B.E., Roy, S.K., Bandyopadhyay, B.C., 2022. Hypercalciuria switches Ca(2+) signaling in proximal tubular cells, induces oxidative damage to promote calcium nephrolithiasis. Genes Dis. 9, 531–548.
Stoeva, M.K., Garcia-So, J., Justice, N., Myers, J., Tyagi, S., Nemchek, M., McMurdie, P. J., Kolterman, O., Eid, J., 2021. Butyrate-producing human gut symbiont, , and its role in health and disease. Gut Microb. 13.
Tang, X., Sun, Y., Li, Y., Ma, S., Zhang, K., Chen, A., Lyu, Y., Yu, R., 2022. Sodium butyrate protects against oxidative stress in high-fat-diet-induced obese rats by promoting GSK-3β/Nrf2 signaling pathway and mitochondrial function. J. Food Biochem. 46, e14334.
Türk, C., Petřík, A., Sarica, K., Seitz, C., Skolarikos, A., Straub, M., Knoll, T., 2016. EAU guidelines on interventional treatment for urolithiasis. Eur. Urol. 69, 475–482.
van den Berg, F.F., van Dalen, D., Hyoju, S.K., van Santvoort, H.C., Besselink, M.G., Wiersinga, W.J., Zaborina, O., Boermeester, M.A., Alverdy, J., 2021. Western-type diet influences mortality from necrotising pancreatitis and demonstrates a central role for butyrate. Gut 70, 915–927.
Wang, G., Qin, S., Chen, L., Geng, H., Zheng, Y., Xia, C., Yao, J., Deng, L., 2023. Butyrate dictates ferroptosis sensitivity through FFAR2-mTOR signaling. Cell Death Dis. 14, 292.
Wang, L., Chen, W., Peng, Z., Liu, C., Zhang, C., Guo, Z., 2015. Vorinostat protects against calcium oxalate-induced kidney injury in mice. Mol. Med. Rep. 12, 4291–4297.
Wang, R., Yang, X., Liu, J., Zhong, F., Zhang, C., Chen, Y., Sun, T., Ji, C., Ma, D., 2022. Gut microbiota regulates acute myeloid leukaemia via alteration of intestinal barrier function mediated by butyrate. Nat. Commun. 13, 2522.
Witting, C., Langman, C.B., Assimos, D., Baum, M.A., Kausz, A., Milliner, D., Tasian, G., Worcester, E., Allain, M., West, M., Knauf, F., Lieske, J.C., 2021. Pathophysiology and treatment of enteric hyperoxaluria. Clin. J. Am. Soc. Nephrol. : CJASN 16, 487–495.
Xu, Y.H., Gao, C.L., Guo, H.L., Zhang, W.Q., Huang, W., Tang, S.S., Gan, W.J., Xu, Y., Zhou, H., Zhu, Q., 2018. Sodium butyrate supplementation ameliorates diabetic inflammation in db/db mice. J. Endocrinol. 238, 231–244.
Yang, C., Ouyang, L., Wang, W., Chen, B., Liu, W., Yuan, X., Luo, Y., Cheng, T., Yeung, K. W.K., Liu, X., Zhang, X., 2019. Sodium butyrate-modified sulfonated polyetheretherketone modulates macrophage behavior and shows enhanced antibacterial and osteogenic functions during implant-associated infections. J. Mater. Chem. B 7, 5541–5553.
Zanger, U.M., Schwab, M., 2013. Cytochrome P450 enzymes in drug metabolism: regulation of gene expression, enzyme activities, and impact of genetic variation. Pharmacol. Therapeut. 138, 103–141.
Zhang, C., Wang, X., Pi, S., Wei, Z., Wang, C., Yang, F., Li, G., Nie, G., Hu, G., 2021. Cadmium and molybdenum co-exposure triggers autophagy via CYP450s/ROS pathway in duck renal tubular epithelial cells. Sci. Total Environ. 759, 143570.
Zhang, Z., Bai, Q., Chen, Y., Ye, L., Wu, X., Long, X., Ye, L., Liu, J., Li, H., 2018. Conditionally reprogrammed human normal bronchial epithelial cells express comparable levels of cytochromes p450 and are sensitive to BaP induction. Biochem. Biophys. Res. Commun. 503, 2132–2138.
Zheng, S., Jin, X., Chen, M., Shi, Q., Zhang, H., Xu, S., 2019. Hydrogen sulfide exposure induces jejunum injury via CYP450s/ROS pathway in broilers. Chemosphere 214, 25–34.
Zhou, B., Te, B., Wang, L., Gao, Y., He, Q., Yan, Z., Wang, H., Shen, G., 2022. Combination of sodium butyrate and probiotics ameliorates severe burn-induced intestinal injury by inhibiting oxidative stress and inflammatory response. Burns : journal of the International Society for Burn Injuries 48, 1213–1220.
Zisman, A.L., Coe, F.L., Cohen, A.J., Riedinger, C.B., Worcester, E.M., 2020. Racial differences in risk factors for kidney stone formation. Clin. J. Am. Soc. Nephrol. : CJASN 15, 1166–1173.
Zorov, D.B., Juhaszova, M., Sollott, S.J., 2014. Mitochondrial reactive oxygen species (ROS) and ROS-induced ROS release. Physiol. Rev. 94, 909–950.